In terms of the Poisson ratio the results quoted in eq 22 can be expressed as

$$\sigma_{27\ °C} = 0.318 \pm 0.023$$
$$\sigma_{73\ °C} = 0.378 \pm 0.006 \quad (23)$$

In conclusion, it appears that in Θ conditions the Poisson ratio σ of a polymer gel is equal to zero within experimental error. This is the behavior to be expected from polymer coils obeying Gaussian statistics.

In a good solvent, on the other hand, the experimental results presented here suggest that the polymer coil is less compressible than is implied by the Flory expression for the free energy. It should, however, be emphasized that the measurements were made on unswollen gels; that is, although their thermodynamic state is well defined (as witnessed by the scaling-law variation of E with polymer concentration[9]), there is overlap between adjacent polymer coils. However, in the absence of measurements on swollen gels, such an explanation for the observed discrepancy remains speculative for the moment.

Acknowledgment. We thank Y. Ayant for helpful conversations and express our gratitude to R. Nossal for his very constructive criticisms of the original text.

References and Notes

(1) P. G. de Gennes, *Macromolecules*, **9**, 587, 594 (1976).
(2) M. Daoud and G. Jannink, *J. Phys. (Paris)*, **37**, 973 (1976); F. Brochard and P. G. de Gennes, *Macromolecules*, **10**, 1157 (1977).
(3) M. Daoud, J. P. Cotton, B. Farnoux, G. Jannink, G. Sarma, H. Benoit, R. Duplessix, C. Picot, and P. G. de Gennes, *Macromolecules*, **8**, 804 (1975).
(4) J. P. Cotton, M. Nierlich, F. Boué, M. Daoud, B. Farnoux, G. Jannink, R. Duplessix, and C. Picot, *J. Chem. Phys.*, **65**, 1101 (1976).
(5) J. P. Munch, S. Candau, J. Herz, and G. Hild, *J. Phys. (Paris)*, **38**, 971 (1977).
(6) A. Belkebir-Mrani, J. E. Herz, and P. Rempp, *Makromol. Chem.*, **178**, 485 (1977).
(7) E. Geissler and A. M. Hecht, *J. Phys. (Paris)*, **39**, 955 (1978).
(8) S. J. Candau, C. Y. Young, T. Tanaka, P. Lemaréchal, and J. Bastide, *J. Chem. Phys.*, **70**, 4694 (1979).
(9) A. M. Hecht and E. Geissler, *J. Phys. (Paris)*, **39**, 631 (1978).
(10) R. A. Gelman and R. Nossal, *Macromolecules*, **12**, 311 (1979).
(11) T. Tanaka, L. O. Hocker, and G. B. Benedek, *J. Chem. Phys.*, **59**, 5151 (1973).
(12) P. J. Flory, "Principles of Polymer Chemistry", Cornell University Press, Ithaca, N.Y., 1967.
(13) M. Daoud and P. G. de Gennes, *J. Phys. (Paris)*, **38**, 85 (1977).
(14) T. Tanaka, S. Ishiwata, and C. Ishimoto, *Phys. Rev. Lett.*, **38**, 771 (1977).
(15) R. Nossal, *J. Appl. Phys.*, **50**, 3105 (1979).
(16) When the temperature of the gel is lowered, there is a small degree of syneresis between the gel and the confining glass cell. The principal effect of this is to dampen the standing mode observed; the frequency, however, remains unchanged. It must be concluded that the slippage occurring at the boundary is not sufficient to change the nature of the mode.
(17) L. D. Landau and E. M. Lifshitz, "Theory of Elasticity", Pergamon Press, Oxford, 1970, Chapter 3.
(18) A. M. Hecht and E. Geissler, *Polymer*, in press.

Dynamics of Semiflexible Polymers in Solution

D. W. Schaefer*†

Sandia National Laboratories,† Albuquerque, New Mexico 87185

J. F. Joanny and P. Pincus

Department of Physics, University of California at Los Angeles, Los Angeles, California 90024. *Received November 30, 1979*

ABSTRACT: The statistical properties of semiflexible polymers are analyzed throughout the temperature–concentration plane above the Θ temperature. At intermediate (semidilute) and high concentrations, polymers which are stiff on the scale of a few monomers are found to differ from completely flexible chains. For semiflexible chains, scaling methods have limited validity compared to completely flexible chains. Mean-field methods are found to be appropriate to most semiflexible systems of intermediate-solvent quality. Experimental data are presented on dilute, semidilute, and concentrated solutions of polystyrene in tetrahydrofuran, ethyl acetate, and methyl ethyl ketone, representing good and marginal solvents. The dilute-solution data are used to characterize independent chain statistics and this information is then used to generate the appropriate temperature–concentration diagram covering higher concentrations. In semidilute solution, predicted crossovers are observed in the concentration dependence of dynamical properties. At volume fractions approaching unity, however, dynamical properties become concentration independent and do not show Θ-like scaling observed in small-angle scattering and predicted by mean-field theory. This discrepancy is attributed to the limited width of the Θ-like regime and to differences in the statistical averages being probed in dynamic vs. static techniques.

I. Introduction

A considerable body of evidence indicates that the properties of chain molecules in solution do not change smoothly as a function of density ρ.[1] Rather a distinct change in behavior is observed at the monomer density ρ^* at which the domains of individual molecules overlap. For example, the radius of gyration, R_g, of a single chain is nearly independent of density for $\rho < \rho^*$ but scales as a power of ρ for $\rho > \rho^*$ ($R_g \sim \rho^{-z}$) where the scaling exponent z is 0.125 for polymers dissolved in good solvents. In this work we study the density dependence of the dynamics of semiflexible chain molecules in good and marginal solvents. In good solvents, we find behavior expected on the basis of scaling concepts, consistent with the experiment of Adam and Delsanti.[2] In the case of marginal solvents, however, we postulate a new regime in the temperature–concentration diagram where the system is more

† A U.S. Department of Energy facility.

0024-9297/80/2213-1280$01.00/0

accurately described by mean-field theory.

For simplicity, we treat the properties of a single chain in dilute solution ($\rho < \rho^*$) before treating the more complicated semidilute case ($\rho > \rho^*$). In section II, we introduce the concept of a temperature-dependent length ξ_τ characteristic of a single chain and establish a more precise definition of good, marginal, and Θ solvents. We further analyze experimental data on the diffusional properties of polymers in dilute solutions to establish the quality of several solvents for polystyrene near room temperature. In section III, we consider semidilute and concentrated systems and define several regions in a temperature–concentration diagram according to the appropriate theory describing chain statistics. We argue that, whereas scaling arguments are appropriate for good solvents, the existence of two characteristic lengths in marginal and Θ solvents invalidates scaling assumptions. Rather, mean-field methods are appropriate to these conditions. In sections IV and V, we analyze experimental data, obtained from light scattering on the dynamics of gellike cooperative modes in semidilute solution. We observe the predicted crossover from good to marginal conditions as a function of density. We find agreement with scaling theories under good-solvent conditions and find near agreement with mean-field theory in the marginal case. At very high densities we find evidence for a third regime where the dynamical properties become concentration independent.

II. Dilute Solutions

In this section, we review the statistical properties of an isolated chain and establish a precise definition of solvent quality. We are particularly concerned with the dependence of the chain dimensions on temperature (or equivalently solvent quality) and molecular weight.

Consider an isolated polymer chain of N monomers dissolved in a solvent such that the effective interaction between monomers is described by an excluded volume v given in virial theory[3] by

$$v = \int [1 - e^{-\beta V(r)}]\, \mathbf{dr} \tag{1}$$

where $\beta = (kT)^{-1}$ and $V(r)$ is the solvent-mediated interaction between a pair of monomers separated by a distance r. The parameter v is temperature dependent and for any reasonable $V(r)$ is proportional to the monomer volume a^3 for completely flexible chains at high temperature and is negative at low temperature. The temperature at which $v = 0$ is called the Θ temperature, at which point the effective two-body interaction between monomers vanishes. For T near Θ, the expansion of eq 1 indicates that v has the approximate form

$$v \sim a^3[(T - \Theta)/T] = a^3\tau \tag{2}$$

Real chains are not completely flexible but are usually stiff on the scale of several monomers. A simple model[4,5] which includes this local rigidity is that of chains which are composed of n monomers arranged in rodlike segments of persistence length b. The persistence chain is then approximated as a sequence of rods of length b where the number of monomers per rod, $n = b/a$, may be of the order of 10. The excluded volume per rod has been shown by Onsager[6] to be b^2a, so we can assume that the temperature dependence of v takes the form of eq 3. At the Θ temperature ($\tau = 0$) a given chain is ideal with a radius given by the random flight result

$$v \sim b^2a\tau = n^2a^3\tau \tag{3}$$

$$R_\Theta = (Nab)^{1/2} \tag{4}$$

At temperatures higher than Θ, excluded-volume effects become important and the chain is swollen.

The statistical properties of the chain in the swollen state have been worked out by Flory[7] in the mean-field approximation. The virial expansion of the free energy F for a single polymer coil is related to v as

$$\beta F = \frac{3R^2}{2R_\Theta^2} + \frac{v}{2n^2}\int \rho^2(r)\, \mathbf{dr} + \ldots \tag{5}$$

where R is the actual coil radius and $\rho(r)$ is the local monomer density. Therefore, $\rho(r)/n$ is the density of rodlike segments at a distance r from the center of mass of the coil. The first term in eq 5 is an entropic contribution from coil expansion; the second term is the excluded-volume interaction augmented by an entropy of mixing.

In the mean-field approximation $\rho(r)$ is a constant and

$$\beta F = \frac{3R^2}{2R_\Theta^2} + \frac{vN^2}{2n^2R^3} \tag{6}$$

The equilibrium radius R of a polymer chain is obtained by minimizing the free energy

$$R_F = N^{3/5}\tau^{1/5}n^{1/5}a \tag{7}$$

That the radius R_F scales as $N^{3/5}$ and not as $N^{1/2}$ as for a Gaussian chain demonstrates the nonperturbative effect of excluded volume as applied to polymers in good solvents ($\tau \gg 0$).

Equation 7 does not differ from Flory's original expression except by definition of parameters. The derivation used here, therefore, suffers from the well-known limitations of the Flory calculation. In particular, the first term of the right-hand side of eq 6 is based on Gaussian chain statistics and therefore overestimates the entropic contribution to the free energy. The second term, however, overestimates the enthalpic contribution to the free energy since the monomer positions are assumed to be uncorrelated. Since real polymers closely follow the $N^{3/5}$ dependence predicted by eq 7, the overestimates of the entropic and enthalpic contributions apparently cancel each other.

Additional limitations of the approach presented here arise due to the form of the excluded volume v used in eq 1 and 3. The expressions treat the chain as a gas of monomers and explicitly ignore the connectedness of the chain. This assumption, however, is not serious since more sophisticated treatments[8] show that the true virial coefficients have the same properties as the gaseous counterparts. Equation 3 may be used, therefore, provided a^3 and Θ are considered as parameters which are not necessarily either the monomer volume or the temperature at which v in eq 1 vanishes. There is ample evidence that Θ points exist where the effective two-body interaction vanishes, but the true Θ point is not simply related to $V(r)$ as implied by eq 1. In fact, two-body interactions persist at the Θ point but these are exactly compensated by higher order interactions.

Comparison of eq 7 with the thermodynamic expression[7] for R_F shows that n is related to the entropy of dilution and is dependent on solvent entropy as well as chain stiffness. In what follows the detailed interpretation of the parameter n is not necessary, so for conceptual simplicity we refer to it as a stiffness parameter and ignore the solvent entropy effect.

The validity of eq 7 depends on the depth of the free energy minimum and effectively requires $\beta F(R_F) \gg 1$ or, using eq 6 and 7

$$N \gg N_\tau \equiv a^6n^7/v^2 \tag{8}$$

$$= n^3/\tau^2 \tag{9}$$

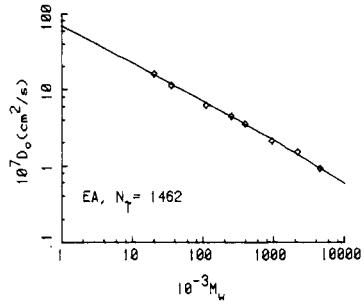

Figure 1. Molecular-weight dependence of the diffusion constant at 25 °C of polystyrene (PS) in ethyl acetate (EA) at infinite dilution. The line is a best fit to the data using the blob model developed by Akcasu and Han.[13]

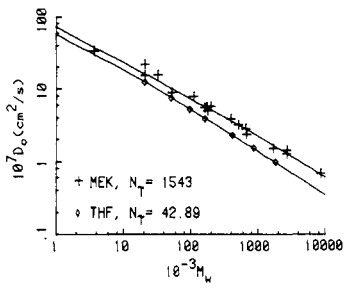

Figure 2. Molecular-weight dependence at 25 °C of the diffusion constant of polystyrene in methyl ethyl ketone (MEK)[12] and tetrahydrofuran (THF).[11] The line is a best fit to the data using the blob model developed by Akcasu and Han.[13]

The inequality expressed by eq 8 permits a more precise definition of solvent quality in terms of degree of polymerization N and temperature

$$\begin{aligned} N \gg N_\tau &\leftrightarrow \text{good solvent} \leftrightarrow \tau \gg (n^3/N)^{1/2} \\ N \ll N_\tau &\leftrightarrow \Theta \text{ solvent} \leftrightarrow \tau \ll (n^3/N)^{1/2} \\ N \simeq N_\tau &\leftrightarrow \text{marginal solvent} \leftrightarrow \tau \simeq (n^3/N)^{1/2} \end{aligned} \tag{10}$$

An alternative way[9] to visualize this result is to consider thermal "blobs" of radius ξ_τ. For length scales much less than ξ_τ, the chain is nearly Gaussian (the excluded-volume effects are small) while for length scales larger than ξ_τ interactions build up to create chain expansion. ξ_τ is then given by eq 4 with $N = N_\tau$

$$\xi_\tau \sim n^4 a^4 v^{-1} = n^2 a \tau^{-1} \tag{11}$$

The blob concept assumes that the chain is sufficiently long that end effects are unimportant. In this case, a chain with $N \gg N_\tau$ can be thought of as a sequence of blobs or renormalized monomers of radius ξ_τ. The renormalized chain will show excluded volume behavior so that

$$R_F = (N/N_\tau)^{3/5} \xi_\tau = N^{3/5} \tau^{1/5} n^{1/5} a \tag{12}$$

where N/N_τ is the number of thermal blobs per chain. Equation 12 indicates that the blob picture gives the same radius as the minimization of the free energy (eq 7). Note that near the Θ point $\tau \to 0$ and $N_\tau \to N$, whereas for a good solvent, $\tau \simeq 1$ and $N_\tau = n^3$, which may be considerably smaller than N.

Recent computer simulations[10] indicate that the blob model severely underestimates the swelling for short internal sequences. In fact, interaction of monomers within an internal sequence with monomers external to the sequence leads to nonideal behavior within a blob. In this work we apply the blob model only in cases where the internal expansion effect is absent: to the overall radius in dilute solution and to internal sequences in semidilute solution. In the latter case, the presence of other chains leads to a screening effect so that the swelling of internal sequences is expected to be absent (see below).

The above discussion indicates the importance of N_τ in the physics of polymer systems. N_τ could be obtained from the crossover in the molecular-weight dependence of any property sensitive to overall chain expansion, such as viscosity, diffusion, or radius of gyration. In fact, the expected crossovers from ideal to excluded-volume behavior seems to be too gradual to permit such an analysis. Figures 1 and 2, for example, show the molecular-weight dependence of the diffusion constant D_0 at infinite dilution of polystyrene (PS) in ethyl acetate (EA), tetrahydrofuran (THF),[11] and methyl ethyl ketone (MEK).[12] In this case, D_0 is expected to scale as R^{-1}, but clearly there is no distinct break in the curve. Fortunately, Akcasu and Han[13] have worked out the complete N dependence of D_0 within the blob model. Application of their analysis permits extraction of N_τ (or equivalently n^3/τ^2) by fitting the data in Figures 1 and 2 to their eq 22. The results of such an analysis are tabulated in Table I. Akcasu and Han's theory was developed for completely flexible chains but the results transform directly to semiflexible systems, provided eq 8 is used to define N_τ and provided $\xi_\tau \gg b$.

Table I
Parameters Obtained by Fitting the Data in Figures 1 and 2 to the Blob Model of Akcasu and Han[13]

solvent	N_τ	τ	n	L, Å
EA	1462	0.232[35]	4.3	8.52
MEK	1543	(0.4)	6.3	9.24
THF	42.9	(0.4)	1.9	9.63

The value of n found for THF is very reasonable in view of the chemical structure of the polystyrene chain. This suggests that the properties of the PS–THF systems will be accurately represented by the semiflexible model. In the case of EA and MEK, however, n is unreasonably large, so it is safe to say that the large value of N_τ is due to an anomalously small excluded volume v rather than chain stiffness. Since insufficient data are available to separate the chain vs. solvent entropy effects, the latter is ignored in the data analysis which follows.

The value of the crossovers obtained from dilute-solution data is expected to depend on the particular type of radius mean value, which is important for the property analyzed. Diffusional measurements are more sensitive to shorter segments than the usual radius of gyration obtained by elastic light or neutron scattering.[14] Diffusional data are used here because they are available for the solvents of interest and because analogous diffusion measurements were carried out on semidilute and concentrated systems. In principle, the same N_τ should be obtained from all types of measurements.

III. Semidilute and Concentrated Solutions

As a polymer solution is concentrated, an overlap density $\rho^* \approx N/R^3$ is reached where the coils begin to entangle. The region $\rho^* < \rho < b^{-3}$ is called the semidilute regime. For $N > N_\tau$, eq 7 yields

$$\rho^* a^3 \sim N^{-4/5} n^{3/5} a^{9/5} v^{-3/5} = N^{-4/5} n^{-3/5} \tau^{-3/5} \tag{13}$$

The exponent $-4/5$ in the molecular-weight dependence of ρ^* is typical of good-solvent behavior. By contrast, in a Θ solvent, $R \sim N^{1/2}$ so that

$$\rho^* a^3 \sim N^{-1/2} n^{-3/2} \tag{14}$$

In the crossover region R does not display simple power dependence on N, so consequently ρ^* also does not show

simple power law dependence on N. This behavior is characteristic of a marginal solvent.

A. Scaling in Good and Θ Solutions. For $\rho > \rho^*$ an additional length scale ξ_ρ comes into the problem.[1,15] ξ_ρ is the range of the monomer–monomer correlation function $g(r)$ or, alternately, is proportional to the mean distance between interchain contacts. ξ_ρ decreases with density since the presence of other chains decreases the range of monomer-pair correlations. In good solvents, therefore, chain statistics depend on the length scale. At distances smaller than ξ_ρ (and larger than ξ_τ) excluded-volume interactions swell the chain. At larger length scales, however, excluded-volume interactions are screened due to neighboring chains and the statistics are ideal.

The correlation length ξ_ρ can be calculated by scaling methods since ξ_ρ must be independent of N for $\rho > \rho^*$ and must be equal to the radius of gyration of independent chains when $\rho = \rho^*$. These two conditions along with a scaling form of ξ_ρ yield[1]

$$\xi_\rho \sim n^{1/4}v^{-1/4}a^{-1/2}\rho^{-3/4} = a(a\rho^3)^{-3/4}n^{-1/4}\tau^{-1/4} \quad (15)$$

Under Θ conditions ($\tau = 0$) scaling might also be expected to apply and a similar analysis leads to

$$\xi_\rho^{\,\Theta} \sim a(\rho a^3)^{-1}n \quad (16)$$

It is the ρ dependence of the characteristic length ξ_ρ which is important in the work to follow. Later we show that ξ_ρ can be determined either from the static structure factor measured by small-angle X-ray or neutron scattering measurements or from the dynamic structure factor obtained from quasi-elastic light scattering.

The scaling analysis reviewed above indicates that $\xi_\rho \sim \rho^{-x}$, where the scaling exponent is $^3/_4$ or 1 at good or Θ conditions. In the following section, we show that in real semiflexible systems scaling methods break down above a second critical density $\tilde{\rho}$ where the temperature-dependent length ξ_τ becomes comparable to ξ_ρ. Later we also suggest that scaling methods are inapplicable in Θ systems, also due to the existence of two-length scales.

B. Mean-Field Theory for Marginal Solutions. The scaling analysis of semidilute good solutions presumes that the chain displays excluded-volume statistics for distances small compared to ξ_ρ. For real systems, however, it is clear that a certain density $\tilde{\rho}$ will be reached where $\xi_\rho = \xi_\tau$ or, from eq 11 and 15, when

$$\tilde{\rho}a^3 \sim n^{-5}a^{-3}v = \tau/n^3 \quad (17)$$

For $\rho > \tilde{\rho}$ a chain is nearly ideal on all length scales. Since the system displays two comparable characteristic lengths near $\tilde{\rho}$, it is not surprising that scaling methods break down. We refer to the regime $\tilde{\rho} < \rho < b^{-3}$ as a marginal semidilute system since a polymer in a dilute marginal solvent ($N \simeq N_\tau$) will entangle at $\rho = \tilde{\rho} = \rho^*$. In good solvents, $\tilde{\rho} > \rho^*$ so that scaling is expected for $\rho^* < \rho < \tilde{\rho}$.

For $\rho < \tilde{\rho}$, $\xi_\rho > \xi_\tau$ and properties dependent on long-wavelength Fourier components are dominated by the length ξ_ρ, whereas short-range properties are determined by ξ_τ. In this latter case, ξ_τ is expected to follow eq 11 since interchain contacts are negligible and short pieces of chain are in a dilute environment. In the opposite regime, $\rho > \tilde{\rho}$, ξ_τ is no longer a critical length scale and the system properties are fixed by ξ_ρ and b and by a new length derived below.

Since the chains are nearly ideal on all length scales in the semidilute marginal system, it is reasonable to treat the weak excluded-volume interactions as a perturbation of an otherwise ideal system. Linear response[16,17] theory provides such a perturbation approach wherein the pair-correlation function is obtained from analysis of the linear change in density when the system is subjected to a weak external potential.

Before treating the excluded-volume perturbation, we first consider the response of an ideal system where chain statistics are dominated by entropic forces. The ideal-chain pair-correlation function $g_0(r)$ takes the form of eq 18 for a semiflexible chain, where Q is the partition

$$g_0(r) = \langle c(r)c(r')\rangle_0 = \frac{1}{Q}\sum_{i,j=1}^{N}\int \delta(r - r_i)\delta(r' - r_j)e^{-\beta H_0(r)}\,d\mathbf{r}^N \quad (18)$$

$$d\mathbf{r}^N \equiv d\mathbf{r}_1 \ldots d\mathbf{r}_N$$

function and $c(r)$ is the density of rodlike segments at point r: $c(r) = \rho(r)/n$. Equation 18 is exact but cannot be solved as written since the Hamiltonian appearing in the Boltzmann factor is not known. Equation 18 need not be solved directly, however, since $g_0(r)$ is already known from random-walk theory[18,19] (see below).

If the ideal system described by eq 18 is subjected to weak external potential $\delta\phi(r) \equiv \sum_j \delta\phi_j(r_j)$, then the density in the presence of $\delta\phi$ will be

$$\langle c(r)\rangle = \langle \sum_i c_i(r)\rangle = \frac{1}{Q}\sum_i \int \delta(r - r_i)\,\exp[-\beta H_0 - \beta\sum_j \delta\varphi_j(r_j)]\,d\mathbf{r}^N \quad (19)$$

or after expansion and Fourier transformation

$$\langle \delta c(K)\rangle = \langle c(K)\rangle - \langle c(K)\rangle_0 = -\chi_0(K)\delta\phi(K) \quad (20)$$

$$\chi_0(K) = \beta\int \exp[-i\mathbf{K}\cdot\mathbf{r}]g_0(r)\,d\mathbf{r} \quad (21)$$

$\chi_0(K)$ is the ideal chain response function. Equation 21 shows that χ is proportional to the Fourier transform of the pair-correlation function which is called the structure factor $S(K)$.

$$\chi_0(K) = \beta S_0(K) = \frac{12\beta c}{K^2 b^2} \qquad R_g^{-1} \ll K \ll b^{-1} \quad (22)$$

The K^{-2} scaling of the ideal structure factor is taken from Debye,[19] who obtained $S_0(K)$ on the basis of random-flight statistics. Equation 21 then implies that $g_0(r)$ has the form $g_0(r) \sim r^{-1}$.

In the presence of weak excluded-volume interactions, an equation like eq 19 follows with additional contributions to the free energy of the form

$$\delta\phi_e = kT\sum_j (v + wc_j)\delta c_j = kT(v + wc)\delta c \quad (23)$$

where $v \approx b^2 a$ and $w \approx a^3 b^3$ are the second and third virial coefficients.[20] Equation 23 represents a mean-field approximation since preaveraged rather than instantaneous concentrations are used. Since $\delta\phi_e$ is assumed small, an additional term appears in eq 20

$$\langle \delta c(K)\rangle = -\chi_0(K)[\delta\phi(K) + kT(v + wc)\delta c(K)] \quad (24)$$

or

$$\langle \delta c(K)\rangle = -\chi(K)\delta\phi(K) \quad (25)$$

with

$$\chi(K) = \frac{\chi_0}{1 + kT(v + wc)\chi_0} = \frac{\beta}{v}\frac{1}{1 + (K\xi_\rho^{\,M})^2} \quad (26)$$

and

$$\xi_\rho^{M} = \frac{b}{(vc + wc^2)^{1/2}} = \frac{an^{1/2}}{(\tau\rho a^3 + \rho^2 a^6)^{1/2}} \quad (27)$$

The new response function $\chi(K)$ is related to $g(r)$ and $S(K)$ as in eq 21 or

$$g(r) = \beta^{-1} \int \exp[i\mathbf{K}\cdot\mathbf{r}]\chi(\mathbf{K})\, d\mathbf{K} \sim \frac{1}{r} \exp[-r/\xi_\rho^{M}] \quad (28)$$

$$K \ll \xi^{-1}$$

Equation 28 is the Edwards[15] form of the pair-correlation function generalized to semiflexible chains. Equation 28 contrasts with the r^{-1} form of $g(r)$ for an ideal chain. The analogy between eq 28 and the screened coulomb potential familiar in ionic-solution theory leads to the characterization of ξ_ρ^{M} as a screening length. In the vicinity of $\tilde{\rho}$, ξ_ρ^{M} goes like $1/\rho^{1/2}$ and at $\rho = \tilde{\rho}$ the expected crossover $\xi_\tau = \xi_\rho$ is observed.

It is interesting to note that eq 28 does not predict a smooth crossover to Θ behavior at high density (i.e., where $v \ll wc$). Rather there are two characteristic lengths in the entire mean-field region ($\rho > \tilde{\rho}$). ξ_ρ^{M} given by eq 28 is the range of the monomer pair-correlation function while ξ_ρ given by eq 16 is the mean distance between interchain contact points.[21] Throughout the mean-field region ξ_ρ^{M} is greater than ξ_ρ^{Θ}. The existence of multiple characteristic lengths leads to the conclusion that scaling results cannot be expected in the semidilute–Θ regime. For a completely flexible chain $n = 1$ and $\xi_\rho^{\Theta} = \xi_\rho^{M}$ at high density. The breakdown of scaling under marginal and Θ conditions is therefore a consequence of the local stiffness of real polymers.

The form of eq 27 indicates that the mean-field region may be subdivided into two regions: (1) $wc \ll v$, which we call marginal semidilute, where $\xi_\rho \sim \rho^{-1/2}$, and (2) $wc \gg v$, which we call Θ semidilute, where $\xi_\rho \sim \rho^{-1}$. The crossover between the two regions occurs at $\rho^\dagger$

$$\rho^\dagger a^3 \sim na^3 v/w = \tau \quad (29)$$

C. Pair-Correlation Function in Good-Solvent, Semidilute Solution. The assumptions leading to the mean-field form of the pair-correlation function in eq 28 require that the chains be nearly ideal on all length scales. This assumption is not valid in good solvents since the chains are swollen. In semidilute systems, however, the chains are swollen only over short distances even in good solvents. Since the chains are ideal over large distances (greater than ξ_ρ), linear response theory could be used if a means were available to account for swelling of short segments. Renormalization provides such a mechanism wherein the chain is visualized as an ideal sequence of renormalized monomers of radius ξ_ρ. Since the renormalized chain is nearly ideal with weak interactions between renormalized monomers, the arguments leading to eq 28 follow directly, provided proper adjustments are made in eq 22 and 23 to make them apply to the renormalized chain. In particular, the renormalized ideal response function $\tilde{\chi}_0(K)$ becomes

$$\tilde{\chi}_0(K) = 12\beta c/gK^2\xi_\rho^2 \quad (30)$$

where g is the number of monomers per blob (renormalized monomer) and ξ_ρ is the radius of the blob

$$\xi_\rho = \left(\frac{g}{N_\tau}\right)^{3/5} \xi_\tau \sim c^{-3/4} \quad (31)$$

where the c dependence follows from eq 15. The interaction energy given in eq 23 must also be renormalized to represent the excluded volume $\tilde{v}$ between blobs. Daoud et al.[1] have shown that $\tilde{v}$ is of the form

$$\tilde{v} \sim g^2 v c^{1/4} \quad (32)$$

so that in the absence of three-body interactions eq 26 becomes

$$\tilde{\chi}(K) = \frac{\beta}{\tilde{v}} \frac{1}{1 + (K\xi_\rho)^2} \quad (33)$$

$$K \ll \tilde{\xi}_\rho^{-1}$$

with

$$\tilde{\xi}_\rho = \frac{\xi_\rho}{(12gvc^{5/4})^{1/2}} \sim \xi_\rho \quad (34)$$

Since $g \sim c^{-5/4}$, apart from numerical coefficients, the range $\tilde{\xi}_\rho$ of the pair-correlation function is identical with the length scale ξ_ρ calculated by scaling. The identification of $\tilde{\xi}_\rho$ and ξ_ρ has been made by Daoud et al.[1] for flexible chains, although minor errors exist in the original derivation. Their results are not modified for semiflexible chains.

Transformation of eq 33 leads to a pair-correlation function of the same form as eq 28 in the region $r \gg \xi_\rho$. For $r < \xi_\rho$, however, $g(r)$ is not expected to be of the r^{-1} form indicated by eq 28 since the derivation leading to eq 33 presumed the chains to be ideal for $r < \xi_\rho$. In fact, short segments are swollen in good solvents. The form of $g(r)$ for $r < \xi_\rho$ can be obtained by a simple scaling argument if scaling is assumed for $S(K)$ in the intermediate regime

$$\tilde{S}(K) \sim cg(K\xi_\rho)^y \qquad b^{-1} \gg K \gg \xi\rho^{-1} \quad (35)$$

Since $\tilde{S}$ must be independent of g for $K \gg \xi_\rho^{-1} \sim g^{-3/5}$, the scaling exponent y must be $y = -5/3$. The pair-correlation function follows from eq 28 and 35

$$\tilde{g}(r) \sim r^{-4/3} \qquad b \ll r \ll \xi_\rho \quad (36)$$

The complete pair-correlation function then can be approximated by eq 36 for small r and eq 28 for large r or

$$\tilde{g}(r) \sim r^{-4/3} e^{-(r/\xi_\rho)} \qquad b \ll r \quad (37)$$

This approximate form of the pair-correlation function for semidilute solutions in good solvents will prove useful in the analysis of the dynamic structure factor in the following section.

The above derivations lead to the conclusion that the pair-correlation function $g(r)$ given by eq 28 should apply throughout the semidilute regime, provided $K \gg \xi_\rho^{-1}$ and the appropriate length scale ξ is used: eq 27 for the marginal and Θ solvents and eq 15 for good solvents. Since the structure factor measured in small-angle X-ray and neutron scattering experiments is directly proportional to the response functions in eq 26 and 33, the correlation range is subject to direct experimental study. Later, we show that ξ_ρ can also be obtained from the dynamic structure factor measured by light scattering.

D. Temperature–Concentration Diagram. Having defined numerous crossover densities in the previous sections, it is convenient to collect this information in a temperature–concentration (T–C) diagram. Daoud and Jannink[22] have developed such a T–C diagram for flexible chains and we expand the diagram to cover semiflexible polymers.

For $\tau > 0$ we distinguish five regions:

I. Dilute systems with $\rho < \rho^*$.

II. Good solvent, semidilute with $\rho^* > \rho > \tilde{\rho}$, where ξ_ρ is given by eq 15.

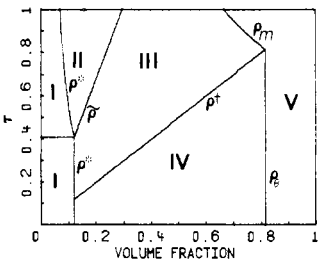

Figure 3. Temperature–concentration diagram for a chain of $N = 20$ monomers with $n = 1.5$ monomers in a persistence length.

III. Marginal solvent, semidilute, where the chains are ideal ($R = (Nab)^{1/2}$) and

$$\xi_\rho \sim \frac{b}{(vc)^{1/2}} = \frac{an^{1/2}}{(\tau\rho a^3)^{1/2}} \tag{38}$$

IV. Θ, semidilute, where

$$\xi_\rho = \frac{b}{(wc^2)^{1/2}} = \frac{an^{1/2}}{\rho a^3} \tag{39}$$

V. Finally a new regime appears where the correlation range becomes comparable to the persistence length

$$\xi_\rho = b \tag{40}$$

We refer to case V as the concentrated region and expect ξ_ρ to be independent of density. The crossover density to regime V depends on solvent quality and can be derived from eq 15, 38, and 39. The crossover occurs at

$$\rho_m a^3 \sim na^3/v = (n\tau)^{-1} \tag{41}$$

from the marginal semidilute to concentrated and at

$$\rho_\theta a^3 \sim n^{-1/2} \tag{42}$$

from semidilute Θ to concentrated solution. No direct crossover from good-solvent semidilute to concentrated solution is found.

The various crossovers are depicted in Figure 3 which is the predicted T–C diagram for semiflexible chains. The major difference between Figure 3 and the T–C diagram for flexible chains is the appearance of the semidilute marginal region III and the concentrated region V. It is important to keep in mind that the various crossovers in Figure 3 are schematic and do not represent "phase" changes. Rather, we expect smooth changes in chain statistics to occur near the indicated crossovers. Moreover, the T–C diagram is qualitative since numerical coefficients have largely been ignored as has the solvent entropy effect. The diagram should be useful in predicting behavior in various solvents but may not be accurate in the absolute crossover concentrations.

Experimental results exist which confirm the general layout of the T–C diagram in Figure 3. In the dilute system (region I) numerous studies confirm the $N^{3/5}$ dependence of the radius of gyration given by eq 7 for a good solvent[23] as well as the $N^{1/2}$ dependence in Θ systems.[24] Neutron scattering data[1] confirm eq 15 for semidilute PS in benzene, a good solvent, whereas X-ray[25] and neutron[26] results confirm the $\rho^{-1/2}\tau^{-1/2}$ dependence of $\xi_\rho^{\,M}$ in eq 27 for PS in MEK and PS in benzene in the marginal regime. Below, we give results obtained by quasi-elastic light scattering which are consistent with Figure 3 in regions II, III, and V.

Computer studies of the end-to-end distance also confirm the existence of a marginal semidilute regime. Curro[27] has collected simulation data from several sources and has tabulated observed scaling exponents for the mean-square end-to-end distance. Generally, these exponents are about −0.1 which lies between the good-solvent value of −0.25 and the marginal value of 0.0 (see Table II). This behavior can be explained on the basis of the local rigidity of a polymer chain on a lattice. In the case of a cubic lattice, for example, $n = {}^3/_2$ so that for relatively short chains the T–C diagram is dominated by the marginal regime even at $\tau = 1$. Figure 3 shows the predicted T–C diagram for $N = 20$ and $n = {}^3/_2$, which is one of the systems studied by Curro. As expected, the good-solvent, semidilute regime between ρ^* and $\tilde{\rho}$ is so small that it is unlikely that scaling predictions would be verified for chains short enough for multichain simulation.

Table II
Predicted Concentration, Molecular-Weight, and Temperature Dependencies of the Radius of Gyration, R_g, and Correlation Range ξ_ρ

	region	R_g^2	ξ_ρ
I.	dilute-Θ	N	
I.	dilute-good	$N^{6/5}\tau^{2/5}$	
II.	semidilute-good	$N\rho^{-1/4}\tau^{1/4}$	$\rho^{-3/4}\tau^{-1/4}$
III.	semidilute-marginal	N	$\rho^{-1/2}\tau^{-1/2}$
IV.	semidilute-Θ	N	ρ^{-1}
V.	concentrated	N	ρ^0

Evidence exists for the semidilute Θ regime from both X-ray and neutron scattering results. Okano et al.,[28] for example, have analyzed SAXS data for PS in MEK near the $\rho^\dagger$ crossover. They analyzed the data by using the complete expression of $\xi_\rho^{\,M}$ in eq 27 and were able to extract both v and w from the measurements. In the case of PS in cyclohexane, Okano et al.[29] have performed a similar analysis SANS data of Cotton et al.[30] and found $\xi \sim \rho^{-1}$ near $\tau = 0$.

The model developed here appears to be consistent with all the structural data observed to date, although no small-angle scattering data yet indicate the existence of the concentrated regime V. Below, dynamic data are analyzed and are found to be consistent with the structural data except in the high-concentration regime where no evidence is found for Θ-like behavior.

IV. Dynamics

Having established the nature of the T–C diagram, we now consider the dynamical properties in semidilute solution. The dynamical properties of entangled polymers in solution depend on the spatial Fourier frequency of the particular displacements being probed.[31] Long-wavelength probes ($KR \ll 1$) such as viscosity reflect the disentanglement or reptation process by which entire chains slither through the entangled mass of polymer. In the opposite limit ($KR \gg 1$) chain motion is internal, so probes such as quasi-elastic neutron scattering will reflect the breathing modes of the polymer chains. In the intermediate regime ($KR \sim 1$) probed by quasi-elastic light scattering, the dynamics reflect gellike longitudinal modes of the system.

The experiments reported below were performed in the pseudogel regime with $KR \sim 1$ and $K\xi_\rho \ll 1$. This system is gellike over short time scales, with the interchain contacts playing the role of temporary cross-links. The segments of chain between contacts behave as dilute polymers of radius ξ_ρ with monomer diffusional motion correlated only over distances comparable to ξ_ρ. The light field scattered by such a system can be written as

$$E(K, t) \sim \sum_J e^{i\mathbf{K}\cdot\mathbf{r}_J} \sum_{j=1}^{g_J} e^{i\mathbf{K}\cdot\mathbf{r}_{Jj}} \tag{43}$$

where $\mathbf{r}_J$ is the center of mass of blob J and the first sum

Table III
Moments of the Distribution of Decay Rates

	mean field, $\nu = {}^1/_2$		scaling, $\nu = {}^3/_5$	
moment	predicted	obsd	predicted	obsd
$\langle\Gamma\rangle$	${}^1/_5\xi \sim \rho^{0.75}$	$\rho^{0.72 \pm 0.15}$	${}^1/_4\xi \sim \rho^{0.5}$	$\rho^{0.40 \pm 0.05}$
$\langle\Delta\Gamma^2\rangle/\langle\Gamma\rangle^2$	0.25	0.37 ± 0.18	0.33	0.55 ± 0.21

is over the number of blobs or renormalized monomers in the system. $\mathbf{r}_{Jj}$ is the vector for the center of mass of blob J to monomer j. g_J is the number of monomers in blob J. Since monomers in different blobs are uncorrelated, the dynamic structure factor becomes ($g_J \gg 1$)

$$S(K, t) \sim \langle E(K, 0)E(K, t)\rangle$$

$$\sim \sum_J g_J^2 \int \exp[i\mathbf{K}\cdot(\mathbf{r}_1 - \mathbf{r}_2)]P(r_1 - r_2; t)\, d\mathbf{r}_1\, d\mathbf{r}_2 \quad (44)$$

The lack of correlated motion between blobs is fundamental to the blob model. This presumption rests on the idea that any hydrodynamic forces which might lead to correlated motion will be screened by the presence of monomers from other chains. This assumption is the dynamic analogue of the static screening concept introduced in eq 28. It is not necessary to assume that the dynamic and static screening lengths are equal but only that they are proportional.

The integral in eq 44 is the Fourier transform of the probability $p(r_1 - r_2; t)$ of observing a monomer at r_2 at time t if some monomer was at r_1 at time zero. The distribution P can be calculated from the diffusion equation for a single chain of radius ξ_ρ to yield

$$S(K, t) = \sum_J g_J^2 \exp\left[-\frac{kT}{\eta r_J}K^2 t\right] \quad (45)$$

where r_J is the radius of blob J and η is the solvent viscosity. Since $g_J \sim r_J^{1/\nu}$, this expression can be written as

$$\frac{S(K, t)}{S(K, 0)} = \int_0^\infty g(r)r^{2/\nu} \exp[(-kT/\eta r)K^2 t]\, d\mathbf{r} \Big/ \int g(r)r^{2/\nu}\, d\mathbf{r} \quad (46)$$

where $g(r)$ is the pair-correlation function given by eq 28 in marginal solvents and by eq 37 in good solvents. The exponent ν is ${}^1/_2$ for marginal and ${}^3/_5$ for good solvents. Since eq 46 is strongly nonexponential, it is convenient to expand the logarithm of eq 46[36]

$$\ln \frac{S(K, t)}{S(K, 0)} = -\langle\Gamma\rangle t + \frac{(\langle\Gamma^2\rangle - \langle\Gamma\rangle^2)t^2}{2\langle\Gamma\rangle^2} + \ldots \quad (47)$$

where $\langle\Gamma^n\rangle$ is the nth moment of the distribution of decay rates Γ

$$\langle\Gamma^n\rangle = \left(\frac{kTK^2}{\eta}\right)^n \int r^{(2-n\nu)/\nu} g(r)\, d\mathbf{r} \Big/ \int r^{2/\nu} g(r)\, d\mathbf{r} \quad (48)$$

The mean-decay rate $\langle\Gamma\rangle$ and the normalized second moment $\langle\Delta\Gamma^2\rangle \equiv (\langle\Gamma^2\rangle - \langle\Gamma\rangle^2)/\langle\Gamma\rangle^2$ are tabulated in Table III. For these calculations $g(r)$ is taken from eq 28 for mean field and eq 37 for scaling. The table indicates that the mean-decay rate is a measure of the correlation range ξ_ρ and that nonexponential correlation functions ($\langle\Delta\Gamma^2\rangle > 0$) are expected throughout the semidilute regime.

V. Experiment

A. Light Scattering. The application of quasi-elastic light scattering to the study of gellike modes in semidilute solution has been extensively analyzed by Adam and Delsanti.[2] Since the technique applied here differs in only minor ways from their work, it is not necessary to discuss methodology extensively. Basically, the dynamic structure factor $S(K, t)$ is obtained by measuring the number of photons $n(t)$ scattered at an angle θ_s in a small time interval centered at time t. A hard-wired computer called a correlator then constructs the photocount correlation function $\langle n(0)n(t)\rangle$ which is directly related to $S(K, t)$

$$\frac{\langle n(0)n(t)\rangle}{\langle n\rangle^2} = 1 + \gamma\frac{S^2(K, t)}{S^2(K, 0)} \qquad t > 0 \quad (49)$$

where γ is a constant of order unity which reflects the degree of spatial coherence of the incident light. The magnitude of the scattering vector K is directly related to the incident wavelength λ, the scattering angle θ_s, and the refractive index n_r

$$K = (4\pi n_r/\lambda)\sin(\theta_s/2) \quad (50)$$

Since the measured correlation functions are strongly nonexponential, the data are analyzed by fitting $\ln[(\langle n(0)n(t)\rangle/\langle n^2\rangle) - 1]^{1/2}$ to a third-order polynomial.[33] The least-squares fitting procedure involves a weighting factor of $[\langle n(0)n(\tau)\rangle - 1]^2$ and the $t \to 0$ limit of the polynomial coefficients yield γ, $\langle\Gamma\rangle$, and $\langle\Delta\Gamma^2\rangle$ which are the lowest order moments of the distribution of decay rates as calculated in section IV.

B. Sample Preparation. It is generally quite difficult to prepare dust-free samples of heavily entangled polymers. We find, however, that it is possible to filter samples up to a molecular weight of about 7×10^6 if the concentration does not exceed the entanglement concentration by more than a factor of 3. Since the measured relaxation rates $\langle\Gamma\rangle$ are independent of molecular weight for semidilute solutions, it is possible to span a large concentration range by studying a range of molecular weights each at a concentration just above entanglement.

Other workers[2] have circumvented the dust problem by using a heterodyne procedure whereby the light scattered by large dust particles acts as a local oscillator. We have avoided this procedure because measured signals are very weak and stability requirements make it virtually impossible to make accurate background subtraction. Since we are concerned with the shape as well as average decay rates of the correlation functions, it is critical that we precisely measure the background $\langle n\rangle^2$ in eq 49.

VI. Results

The previous sections indicate that the mean-decay rate of the photocount correlation function is a measure of the correlation range ξ_ρ in semidilute solution. One of the experimental objectives, then, is to establish the concentration dependence of ξ_ρ in marginal and good solvents and to observe the predicted crossovers $\tilde{\rho}$, $\rho^\dagger$, and ρ_m. Furthermore, since the initial curvature of the measured correlation functions is sensitive to the width of the distribution of decay rates, it is possible to test the predictions for $\langle\Delta\Gamma^2\rangle$ in Table III. Since $\langle\Delta\Gamma^2\rangle$ is dependent on the form of $g(r)$, the experimental data provide a test of the adequacy of the pair-correlation functions in eq 28 and 37.

Figure 4 shows the measured mean-decay rates as a function of concentration for PS in THF at 25 °C. By the definition of eq 49 and the analysis of Figure 1, THF is a good solvent for PS and the chains are expected to be swollen for $N > 42$. From the analysis of section III, therefore, we expect this system to be described by scaling methods throughout most of the concentration domain. In fact, Figure 4, top, shows the T–C diagram, assuming $n = 1.9$ (see Table I). If τ is assumed to be 0.4 for this system (the Θ point is not known), the data in Figure 4, bottom, are taken along the $\tau = 0.4$ line indicated in Figure 4, top. For volume fractions $\phi_v = \rho a^3$ less than about 0.06, scaling behavior is expected with $\langle\Gamma\rangle/K^2 \sim \xi_\rho^{-1} \sim \phi_v^{3/4}$. The solid line in Figure 4, bottom, is drawn for a slope of ${}^3/_4$ and is seen to be consistent with the data for volume fractions less than 0.1. Above $\phi_v = 0.06$ marginal behavior is predicted with $\langle\Gamma\rangle/K^2 \sim \phi_v^{1/2}$. The solid line near $\phi_v = 0.1$ in Figure 4, bottom, is the best fit to the data with

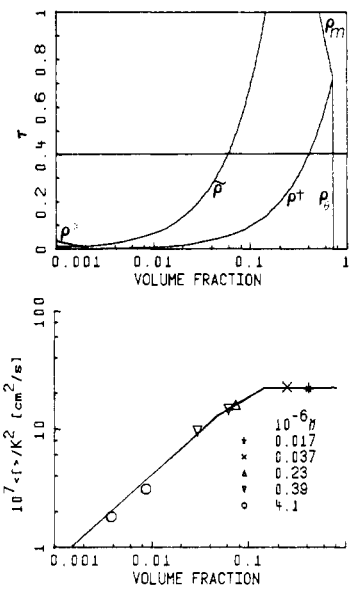

Figure 4. (Top) Temperature–concentration diagram for PS in THF. The parameter n is taken from the molecular-weight dependence of the diffusion constant at infinite dilution as tabulated in Table I. Since the Θ temperature is not known, the horizontal line is an estimate of the appropriate temperature for the data in Figure 4, bottom. τ is not exactly known since the Θ point is below the freezing point of THF. (Bottom) Concentration dependence of the mean-relaxation rate of PS in THF at 25 °C. The lines represent best fits to the data using the slopes predicted by the theory developed here. The large region with slope 0.75 indicates scaling behavior characteristic of a good solvent. Boundaries between the various regions are ill-defined, so the limits of the small marginal regime are somewhat arbitrary.

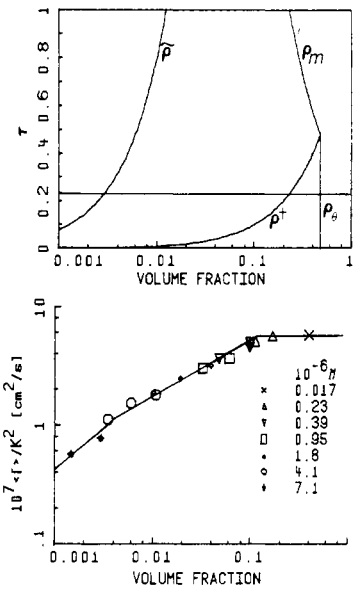

Figure 5. (Top) Temperature–concentration diagram for PS in EA. The horizontal line indicates the appropriate τ for the data in Figure 5, bottom. (Bottom) Concentration dependence of the mean-relaxation rate for PS in EA at 25 °C. The lines represent a best fit, assuming slopes predicted by the theory outlined in this paper. The large mean-field region with slope ≃0.5 indicates EA is a marginal solvent. As indicated, a small scaling region with slope 0.75 may be present at the lowest concentrations and the data become concentration independent at the highest values, indicating the behavior characteristic of a concentrated solution. The data show no indication of Θ behavior, although the temperature–concentration diagram suggests a Θ regime should be present. In the mean-field regime the data slope is actually 0.40 ± 0.05.

a slope of $^1/_2$, and this line is consistent with the data between $\phi_v = 0.06$ and $\phi_v = 0.15$.

The above analysis indicates that both scaling and mean-field behavior are observed in THF, depending on the concentration. The crossover predicted on the basis of section III is observed and the concentration dependence of ξ_ρ is properly predicted. The data do not extend to high enough concentration to establish the semidilute Θ or the concentrated regime, but the extreme high-concentration data point indicates that $\xi_\rho \rightarrow c^0$, so apparently the Θ regime is too narrow to be observed in this system.

Two marginal systems were studied:[34] PS in MEK and PS in EA. Since the data are more extensive in EA, this system is analyzed first in Figure 5. Once again the predicted T–C diagram is displayed above the data with a horizontal line at the appropriate τ.[35] This system is expected to display a small scaling regime at low concentration and a very large mean-field regime. The predicted slopes are indicated in Figure 5, bottom, which shows some indication of the expected crossover at $\phi_v \simeq 0.0015$. In the mean-field regime, the data slope is 0.40 ± 0.05, somewhat less than the expected 0.5, and there is no indication of Θ behavior at high concentration. Once again the semidilute Θ regime is apparently too narrow to be observed at this temperature. The data appear to smoothly breakover to concentration independence at large ϕ_v.

In MEK the situation is very similar to that in EA, as expected on the basis of the T–C diagram shown in Figure 6, top. In this system τ is assumed to be 0.4 so that the $\tilde{\rho}$ and $\rho^\dagger$ crossovers are not expected in this system over the concentration range studied. Rather a large mean-field regime with $\langle\Gamma\rangle/K^2 \sim \phi_v^{1/2}$ is predicted with crossover to concentration independence at $\phi_v \sim 0.4$. The data are generally consistent with this picture except that the slope

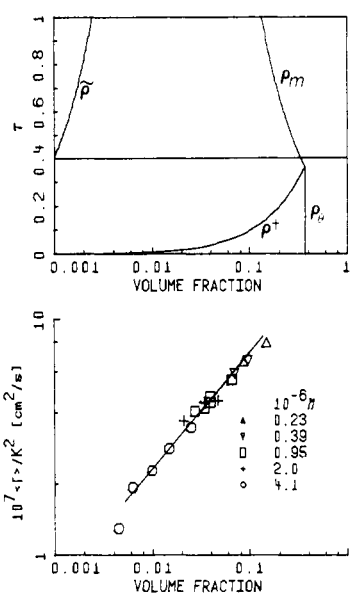

Figure 6. (Top) Temperature–concentration diagram for PS in MEK. The horizontal line represents the approximate conditions for the data in Figure 6, bottom. (Bottom) Concentration dependence of the mean-decay rate for PS in MEK at 25 °C. The line is the best fit to the data, assuming a slope of 0.5 corresponding to mean-field behavior. The slope of the data is actually 0.41 ± 0.07.

is somewhat less than 0.5 and there is a hint of $\tilde{\rho}$ crossover from the lowest concentration data point.

Overall, the mean-decay rates are quite consistent with the model developed here except in the high-concentration regime. Here the data show concentration independence at lower concentrations than expected and there is no

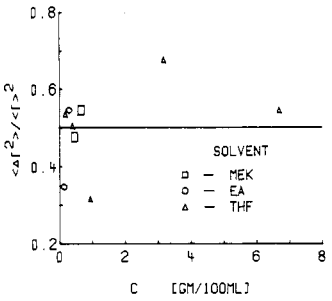

Figure 7. Normalized width of the distribution of decay rates in the good solvent semidilute regime.

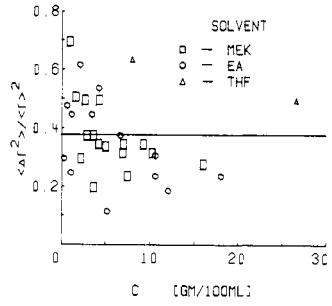

Figure 8. Normalized width of the distribution of decay rates in the semidilute marginal regime.

evidence of Θ-like behavior. The concentration independence is consistent with recent work reported by Patterson et al. in which the dynamics of polystyrene were studied during the polymerization process.[36] The results showed concentration independence but, in addition, these workers observed decreasing relaxation rates at near-bulk concentrations. For these extremely high concentrations, the model developed here is clearly not adequate to describe the system dynamics since chain motion (friction) is no longer dominated by the solvent. As pointed out by Patterson et al., such a system should be viewed as a solid polymer whose glass transition temperature is increasing with concentration.

Analysis of the width $\langle \Delta\Gamma^2 \rangle$ of the distribution of decay rates is somewhat more difficult since errors in the determination of $\langle \Delta\Gamma^2 \rangle$ are of the order of $\langle \Delta\Gamma^2 \rangle$. Therefore, it is appropriate to analyze all the data from the three solvents as a unit. Figure 7, for example, shows all the data between $\tilde{p}$ and $\rho^\dagger$, which is the marginal regime where Table III indicates $\langle \Delta\Gamma^2 \rangle / \langle \Gamma \rangle^2$ should be 0.25. This compares favorably with the experimental value of 0.38 ± 0.18. In the good-solvent regime the data are more limited with an average of $\langle \Delta\Gamma^2 \rangle / \langle \Gamma \rangle^2 = 0.50 \pm 0.21$, which is also consistent with the prediction of 0.33. Thus, the magnitude of $\langle \Delta\Gamma^2 \rangle$ as well as the trend with solvent quality is consistent with the model developed here.

VII. Conclusion

We have attempted to analyze the dynamic properties of polymer chains throughout the temperature–concentration plane. In dilute solution center-of-mass diffusion data are used to define the temperature-dependent quantity N_τ, which characterizes the crossover from ideal to swollen chain statistics. In semidilute solution we find several regions of the T–C plane where the concentration dependence of chain dynamics differ. In most systems, we expect behavior characteristic of good, marginal, or Θ solvents, depending on concentration. At very high densities we expect also to observe a concentrated region where dynamical properties become concentration independent.

The model presented here is consistent with most existing data obtained by quasi-elastic light scattering. Data presented here include both good and marginal systems, and the expected crossover from good to marginal semidilute behavior is observed in all cases. The results of other workers in good solvents are also consistent with the model presented.

In general, semidilute scaling behavior is expected for systems where $v \simeq a^3$ and where the chains are very flexible ($n \sim 1$). By contrast, a large mean-field regime is expected if the chains are stiff on the scale of several monomers or if the effective excluded volume is considerably smaller than the geometric monomer volume.

The power law exponents observed in region III fall detectably below the mean-field prediction. This behavior may be due to a breakdown in the assumption that the system is semidilute. These systems are very congested, and undoubtedly short segment friction is no longer totally dominated by the solvent.

In the moderate-to-high concentration regime, some discrepancies still persist in the interpretation of both static and dynamic measurements. For the systems studied here, relaxation rates become concentration independent near volume fractions of 0.2 and there is no evidence for Θ-like scaling at intermediate concentration in marginal solvents. The origin of this discrepancy is not clear but may result from the fact that the Θ semidilute regime is rather narrow and may not be observable in all systems. In fact, the T–C diagram in Figure 6, top, indicates that Θ behavior is not expected for PS in MEK. It is also possible that static and dynamic measurements will show different behavior and inconsistent crossover points due to the fact that different statistical averages are involved. Dynamic measurements are sensitive to $\langle 1/r \rangle$, where r is the distance between correlated monomers. Static measurements, on the other hand, measure the $\langle r^2 \rangle$ and are therefore more sensitive to the wings of the pair-correlation function. Finally, it is possible that chain friction is no longer dominated by the solvent for systems above volume fractions of 0.2. If this were the case, static and dynamic measurements would not yield the same correlation length. A complete analysis of this problem obviously requires attention to the details of the specific effect being analyzed. Such an analysis is beyond the scope of this paper which is meant to be qualitative in nature. As more data become available, however, such an analysis may be necessary. At present, it is the intermediate- and high-concentration regimes as well as the Θ system which require more extensive experimental work. For the systems studied here, difficulties in preparation of clean samples add uncertainties which limit the accuracy of the intermediate-concentration data and impede definite conclusions concerning the nature of the system at high concentrations. It is hoped nevertheless that problem areas have been sufficiently defined that definitive experiments will be forthcoming.

Acknowledgment. This work was supported by the U.S. Department of Energy under Contract DE-AC04-76-DP00789. J.F.J. and P.P. were supported by the National Science Foundation. We thank R. T. Rotkosky and S. L. Chavez for technical assistance in this work. We have benefited greatly from discussions with J. G. Curro.

References and Notes

(1) M. Daoud, J. P. Cotton, B. Farnoux, G. Jannink, G. Sarma, H. Benoit, R. Duplessix, C. Picot, and P. G. de Gennes, *Macromolecules*, 8, 804 (1975).
(2) M. Adam and M. Delsanti, *Macromolecules*, 10, 1229 (1977).
(3) H. Yamakawa, "Modern Theory of Polymer Solutions", Harper and Row, New York, 1971.
(4) The persistence chain model is obviously a severe approximation but it provides a simple framework to treat real polymers.

Although we do not expect true rodlike characteristics at short length scales, we do expect that properties which are sensitive to distances larger than b will be adequately represented by this model.
(5) O. Kratky and G. Perod, *Recl. Trav. Chim. Pays-Bas*, **68**, 1106 (1949).
(6) L. Onsager, *Ann. N.Y. Acad. Sci.*, **51**, 627 (1947).
(7) P. J. Flory, "Principles of Polymer Chemistry", Cornell University Press, Ithaca, NY, 1953.
(8) A. R. Khoklov, *Polymer*, **19**, 1387 (1978).
(9) B. Farnoux, F. Boue, J. P. Cotton, M. Daoud, G. Jannink, M. Nierlich, and P. G. de Gennes, *J. Phys.* (*Paris*), **39**, 77 (1978).
(10) J. G. Curro, proceedings of symposium dedicated to R. Simha, to be published in *J. Macromol. Sci.*
(11) W. Mandema and Z. Zeldenrust, *Polymer*, **18**, 835 (1977).
(12) T. A. King, A. Knox, and J. D. G. McAdam, *Polymer*, **14**, 293 (1973); N. C. Ford, F. E. Karasz, and J. E. M. Owen, *Discuss. Faraday Soc.*, **49**, 228 (1970); Application Note LS8, Chromatix Corp.
(13) A. Z. Akcasu and C. C. Han, *Macromolecules*, **12**, 276 (1979).
(14) G. Weill and J. des Cloizeaux, *J. Phys.* (*Paris*), **40**, 99 (1979).
(15) S. F. Edwards, *J. Phys. A*, **8**, 1670 (1975).
(16) P. G. de Gennes, *J. Phys.* (*Paris*), **31**, 235 (1970).
(17) G. Jannink and P. G. de Gennes, *J. Chem. Phys.*, **48**, 2260 (1968).
(18) P. J. Flory, "Statistical Mechanics of Chain Molecules", Interscience, New York, 1969, Chapter 9.
(19) P. Debye, *Ann. Phys.*, **46**, 809 (1915).
(20) J. P. Straley, *Mol. Liq. Cryst.*, **24**, 7 (1973).
(21) If the distance between interchain contact points is ξ and the number of monomers between contact points is g, they are related by the two relations

$$g = \rho\xi^3$$

$$\xi = g^{1/2}(ab)^{1/2}$$

The first of these relations expresses the fact that each monomer has to be between two contact points; the second says that between two contact points we have an ideal single-chain behavior. Solving these equations yields $\xi = (\rho ab)^{-1} = \xi_\rho^\theta$
(22) M. Daoud and G. Jannink, *J. Phys.* (*Paris*), **37**, 973 (1976).
(23) Y. Miyaki, Y. Einaga, and H. Fujita, *Macromolecules*, **11**, 1180 (1978).
(24) C. Loucheux, G. Weill, and H. Benoit, *J. Chim. Phys. Phys.-Chim. Biol.*, **43**, 540 (1958).
(25) D. W. Schaefer and R. W. Hendricks, *Polym. Prepr., Am. Chem. Soc., Div. Polym. Chem.*, **20**, 891 (1979).
(26) R. W. Richards, A. Maconnachie, and G. Allen, *Polymer*, **19**, 266 (1978).
(27) J. G. Curro, *Macromolecules*, **12**, 463 (1979).
(28) K. Okano, E. Wada, K. Kurita, and H. Fukuro, *J. Appl. Crystallogr.*, **11**, 507 (1978).
(29) K. Okano, E. Wada, K. Kurita, H. Hiramatsu, and H. Fukuno, *J. Phys. Lett.* (*Paris*), **40**, L-17 (1979).
(30) J. P. Cotton, M. Nierlich, F. Boue, M. Daoud, B. Farnoux, G. Jannink, R. Duplessix, and C. Picot, *J. Chem. Phys.*, **65**, 1101 (1976).
(31) P. G. de Gennes, *Macromolecules*, **9**, 587, 594 (1976).
(32) P. N. Pusey, D. E. Koppel, D. W. Schaefer, R. D. Camerini-Otero, and S. H. Koenig, *Biochemistry*, **13**, 952 (1974).
(33) J. C. Brown, P. N. Pusey, and R. Dietz, *J. Chem. Phys.*, **62**, 1136 (1975).
(34) D. W. Schaefer, *Polym. Prepr., Am. Chem. Soc., Div. Polym. Chem.*, **19**, 733 (1978).
(35) S. Saeki, S. Konno, N. Kawahara, M. Nakata, and M. Kaneko, *Macromolecules*, **7**, 521 (1974).
(36) G. D. Patterson, J. R. Stevens, G. R. Alms, and C. P. Lindsey, *Macromolecules*, **12**, 661 (1979).

Thermal Oligomerization of Bis[4-(3-ethynylphenoxy)phenyl] Sulfone and 4-(3-Ethynylphenoxy)phenyl Phenyl Sulfone

J. M. Pickard* and S. C. Chattoraj

Research Applications Division, Systems Research Laboratories, Inc., Dayton, Ohio 45440

G. A. Loughran and M. T. Ryan

Air Force Materials Laboratory, Air Force Wright Aeronautical Laboratories, Air Force Systems Command, Wright-Patterson Air Force Base, Ohio 45433. *Received March 4, 1980*

ABSTRACT: Infrared, ^{1}H NMR, and ^{13}C NMR characterization data are presented for oligomers isolated from the thermal reaction of bis[4-(3-ethynylphenoxy)phenyl] sulfone (**1**) in the initial stages of reaction and 4-(3-ethynylphenoxy)phenyl phenyl sulfone (**2**) up to 90% conversion. Thermal reaction of each monomer at 434 K yields conjugated oligomers having molecular weights of about 2800 as well as lower molecular weight species presumed to consist of dimer and trimer. The IR spectrum of oligomer **1** and its deuterated analogue exhibit bands at 3290 and 2550 cm^{-1}, respectively, which indicates that pendant ethynyl moieties exist in the oligomer. The presence of unsaturation in both oligomers is indicated by the ^{1}H and ^{13}C NMR spectra. Assignments for the aromatic carbons in the ^{13}C NMR spectra for the oligomers are derived from group additivity and are confirmed for oligomer **2** by changes in the ^{13}C NMR spectrum which are induced by the addition of a shift reagent, Eu(fod)$_3$. Tentative assignments are proposed for the α and β carbons of the polyene chains. It is suggested that both oligomers possess a trans-cisoidal conformation.

Introduction

Thermal polymerization of aromatic and heteroaromatic acetylene-terminated monomers yields condensed resins which possess unique thermooxidative and mechanical properties.[1-3] While the mechanism of the reaction is poorly understood, studies based upon observations involving model compounds and selected monomers have suggested that the principal reaction involves dimerization,[4,5] chain extension,[5] and cyclotrimerization.[5,6] Recently, the complexity of the cure reaction has also been eloquently revealed by Schaefer and co-workers,[7] who demonstrated by magic-angle ^{13}C NMR studies that only

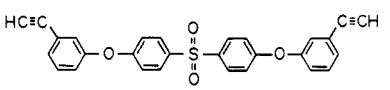

1

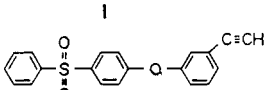

2

about 30% of the ethynyl moieties react by cyclotrimerization. Analogies based upon the reactivity of simpler arylacetylenes[8-11] suggest that the primary reaction in the initial curing stage might be one involving the formation of low-molecular-weight polyenes. In order to

0024-9297/80/2213-1289$01.00/0